Implantation-induced nonequilibrium reaction between Zn ions of $60\,\mathrm{keV}$ and SiO_2 target

H. Amekura, M. Yoshitake, O. A. Plaksin, N. Kishimoto, Ch. Buchal, and S. Mantl

Citation: Appl. Phys. Lett. **91**, 063113 (2007); doi: 10.1063/1.2768004
View online: https://doi.org/10.1063/1.2768004
View Table of Contents: http://aip.scitation.org/toc/apl/91/6
Published by the American Institute of Physics

Implantation-induced nonequilibrium reaction between Zn ions of 60 keV and SiO_2 target

H. Amekura,[a] M. Yoshitake, O. A. Plaksin,[b] and N. Kishimoto
National Institute for Materials Science, 3-13 Sakura, Tsukuba, Ibaraki 305-0003, Japan

Ch. Buchal and S. Mantl
Institut fuer Bio- und Nanosysteme (IBN1-IT), Forschungszentrum Juelich GmbH, D-52425 Juelich, Germany

(Received 15 June 2007; accepted 11 July 2007; published online 7 August 2007)

Silica glass (SiO_2) was implanted with 60 keV Zn^+ ions to a fluence of 1.0×10^{17} ions/cm^2, and the chemical states were investigated along the depth in as-implanted state by x-ray excited Auger electron spectroscopy and x-ray photoelectron spectroscopy. The metallic Zn and Zn_2SiO_4 phases were found to have, respectively, formed in the shallow and deep regions of the SiO_2, whereas thermodynamics predicts the Zn phase only. Oxygen atoms in SiO_2 are preferentially displaced to the deeper region because of the lighter mass. The excess oxygen in the deep region and athermal energy from the implantation drive the formation of Zn_2SiO_4. © *2007 American Institute of Physics*. [DOI: 10.1063/1.2768004]

Over the past several decades, ion implantation has established an important position in semiconductor industry. Recently, various new attempts have been made to achieve nonsilicon nanostructure fabrication using ion implantation. One of these is the formation of metal and semiconductor nanoparticles (NPs) in insulators. In pursuit of higher optical nonlinearity, plasmonic devices, single electron operation, a higher magnetic coercive field, size-dependent luminescence, and ultraviolet (UV) luminescence, various metal and semiconductor NPs have been formed in insulators such as SiO_2 and Al_2O_3 using ion implantation.

In the ion implantation process, ions of usually a few tens to several hundred keV are made to impact a solid-state target material. Because of interactions with the target material, the implanted ions are rapidly decelerated and stop within the surface layer at depths not exceeding a few hundred nanometers. The energy of incoming ions is statistically deposited in nanoscopic regions of the thin surface layer via high-density electron excitation along the ion trajectories and the cascade displacements of constituent atoms in the target.[1] In the course of time, the highly nonequilibrium states formed along the ion tracks are relaxed to quasiequilibrium states where effective lattice temperatures are locally definable but on the order of thousands of kelvins; i.e., thermal spikes.[1] Since the cascade collisions generate a large number of broken bonds and displace atoms away from the stable sites, chemical reactivity in the implanted layer increases. Simultaneously, the high-density electron excitation may also further enhance the reactivity. The thermal spikes may play a role as well. Consequently, chemical reactions with extraordinary efficiency and/or those that never occur in conditions close to thermoequilibrium can be expected in the implanted layers.

In this letter, we report the results of chemical analysis of SiO_2 samples implanted with Zn^+ of 60 keV ions using x-ray photoelectron spectroscopy (XPS) and x-ray excited Auger electron spectroscopy (XAES). While thermodynamics predicts the formation of metallic Zn but not the Zn_2SiO_4 phase, both Zn NPs and Zn_2SiO_4 NPs were observed in the implanted samples. The mechanism of the formation of the Zn_2SiO_4 is discussed.

Samples of KU-1-type optical-grade silica glass (SiO_2) of 15 mm in diameter and 0.5 mm in thickness were implanted in a vacuum chamber, with $^{64}Zn^+$ ions of 60 keV up to a fluence of 1.0×10^{17} ions/cm^2. The ion flux was limited to less than 2 μA/cm^2 in order to maintain the sample temperature (measured by a thermocouple from the rear side) at below 100 °C during implantation. The pressure in the sample chamber was kept at 1×10^{-4} Pa or less during implantation. After the implantation was completed and the samples were allowed to cool down to room temperature (RT), the samples were once exposed to the air, then transferred to an ultrahigh-vacuum XPS chamber. The diffusion constant of oxygen in SiO_2 (Ref. 2) is given by $D(T)=2\times10^{-9}\exp(-E/kT)$(cm^2/s), and D(300 K) is estimated as $\sim10^{-30}$ cm^2/s. The exposure in air at RT does not affect the Zn species because the diffusion constant is too low and all of the implanted Zn species are located inside the SiO_2 matrix.[3,4] All of the samples were examined in the as-implanted state, without any heat treatment. XPS and XAES were carried out using a monochromatic Al $K\alpha$ x-ray source ($h\nu$=1486.7 eV) with an electron neutralizer. Owing to the neutralizer, the samples were mostly free from significant charging. Depth profiling was performed by sputtering using a 1 kV Ar^+ beam.

Figure 1 shows XAES spectra of Zn–$L_3M_{45}M_{45}$ Auger transitions at various sputtering depths. There was little evidence of Zn signal on the surface (0 nm). This is consistent with the results of cross-sectional transmission electron microscopy,[4] showing that all of the Zn nanoparticles are embedded into the substrate. With increasing sputtering depth, two peaks appear at kinetic energies of 992.2 and 995.6 eV, both of which are ascribed to metallic Zn.[5] The metallic peaks grow larger with the depth, reaching a maximum at a depth of ~15 nm and decreasing in deeper regions. A weak peak is visible at 986.1 eV at a depth of 6 nm, which is ascribed to the Zn_2SiO_4 phase. The weak peak coexists

[a]Author to whom correspondence should be addressed; FAX: +81-29-863-5599; electronic mail: amekura.hiroshi@nims.go.jp
[b]Present address: SSC RF, A.I. Leypunsky Institute of Physics and Power Engineering, Obninsk, Kaluga region, 2490033, Russia.

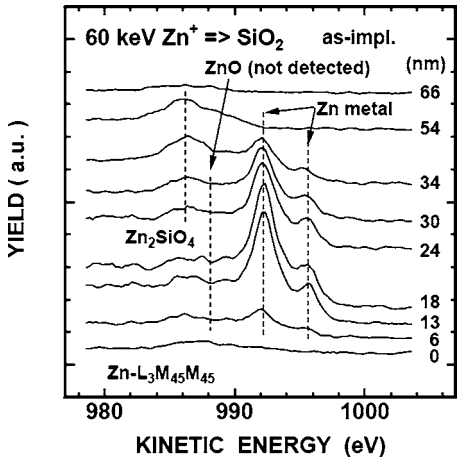

FIG. 1. XAES spectra around $Zn-L_3M_{45}M_{45}$ Auger transitions from a SiO_2 sample in the as-implanted state, which was implanted with 60 keV Zn^+ ions to a fluence of 1.0×10^{17} ions/cm^2. The sputtering depth of each spectrum is indicated on the right-hand side of the figure. Each spectrum is shifted vertically for clarity. The energy positions of Zn, ZnO, and Zn_2SiO_4 species are shown by dashed lines.

with the strong metallic signals. While the metallic signals disappear in the regions deeper than 40 nm, the Zn_2SiO_4 phase shows a maximum at ~42 nm. It should be noted that ZnO signal, which should appear at 988.1 eV,[5] is not observed at any depth. The formation of the Zn_2SiO_4 phase is also confirmed in the Zn $2p_{3/2}$ transition of XPS.

The depth profiles of Zn atoms, which form the metallic Zn and Zn_2SiO_4 phases, are shown in Fig. 2(a). As already mentioned, the Zn and Zn_2SiO_4 phases show concentration maxima at ~15 and ~42 nm, respectively. The ZnO component was below the detection limit. A spatial separation is observed along the depth between the metallic Zn and Zn_2SiO_4 phases; i.e., the Zn and the Zn_2SiO_4 phases are located in shallower and deeper regions, respectively.

In Fig. 2(b), depth profiles calculated in the frame of linear cascade approximation, i.e., by SRIM2003 (Ref. 6) and TRIDYN (Ref. 7) codes, are plotted. The SRIM code neglects the sputtering loss while TRIDYN includes it. The fluence of 1.0×10^{17} ions/cm^2 was so high that the sputtering loss was no longer negligible. In fact, TRIDYN predicted a conspicuously shallower profile than SRIM2003. The profile predicted

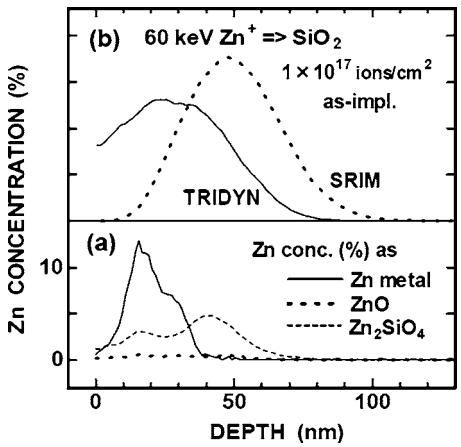

FIG. 2. (a) Concentration profiles along the depth of Zn atoms existing as chemical forms of metallic Zn, ZnO, and Zn_2SiO_4 plotted by solid, dotted, and dashed lines, respectively. (b) Depth profiles of Zn atoms in SiO_2 implanted with 60 keV Zn^+ ions to a fluence of 1.0×10^{17} ions/cm^2 calculated by SRIM2003 and TRIDYN codes, plotted by dotted and solid lines, respectively.

TABLE I. Gibbs free energy changes of the formation reactions of Zn_2SiO_4 at 300 K and extrapolated values to 3000 K. The symbols (○) and (×) represent allowed ($\Delta G^\circ<0$) and forbidden ($\Delta G^\circ>0$) reactions, respectively.

ΔG° (kJ/mol)	T=300 K	$T\rightarrow$3000 K
Without oxygen		
(A) $2Zn+2SiO_2\rightarrow Zn_2SiO_4+Si$	+185 (×)	+153 (×)
With oxygen (O_2 or O)		
(B) $2Zn+SiO_2+O_2\rightarrow Zn_2SiO_4$	−665 (○)	+172 (×)
(C) $2Zn+SiO_2+2O\rightarrow Zn_2SiO_4$	−1129 (○)	+60 (×)

by TRIDYN is similar to the sum of the experimental profiles of Zn metal and Zn_2SiO_4 shown in Fig. 2(a), except that the experimental profile shows a sharp peak at a depth of ~15 nm and lower concentration close to the surface. These differences are probably due to postcollision processes, which are not included in TRIDYN simulation. One might explain the sharp peak by assuming partial loss of Zn atoms located close to the surface. However, no noticeable decrease of Zn content compared to the fluence of implanted ions was observed by the Rutherford backscattering spectrometry. Comparison of the TRIDYN profile and the experimental profiles suggests that the Zn_2SiO_4 phase forms at almost the same depths where Zn atoms are implanted, without long migration.

Table I summarizes possible reactions for the formation of the Zn_2SiO_4 phase from Zn and SiO_2. The simplest reaction is that in which Zn atoms are oxidized by oxygen liberated from the decomposition of SiO_2, i.e.,

$$2Zn + SiO_2 \rightarrow 2ZnO + Si, \quad (1)$$

then the ZnO reacts with SiO_2,

$$2ZnO + SiO_2 \rightarrow Zn_2SiO_4. \quad (2)$$

From the combination of these two reactions, reaction (A) shown in Table I is obtained. Reaction (A) does not proceed spontaneously: the corresponding Gibbs energy change ΔG° at 300 K is +185 kJ/mol; i.e., a positive value. This is because reaction (1) above, the reduction of SiO_2, is characterized by a very high positive change of the free energy.

If oxygen species are supplied from outside, as shown in reactions (B) and (C), in Table I, ΔG° at 300 K gives negative values; i.e., the Zn_2SiO_4 phase is formed. These predictions have also been confirmed by thermal annealing experiments.[4,8] Annealing *in oxygen gas* at 700 °C for 1 h induces the formation of ZnO NPs on the surface of SiO_2 substrate, but not the Zn_2SiO_4 phase. However, after annealing at higher temperature 900 °C for 1 h in oxygen gas, the Zn species is completely transformed to the Zn_2SiO_4 phase covering the surface of SiO_2 substrate.[4] The Zn_2SiO_4 forms *on the surface of* SiO_2 *by annealing*.

It should be noted again that, *under implantation*, the Zn_2SiO_4 phase *embedded in* the SiO_2 is formed in the vacuum chamber of 1×10^{-4} Pa pressure. The residual oxygen in the vacuum chamber is not enough to transform a certain portion of the Zn to Zn_2SiO_4. Even if the Zn_2SiO_4 phase could be formed by reaction with residual oxygen in the vacuum chamber, the Zn_2SiO_4 would form *on the surface of the* SiO_2 since the residual oxygen would be supplied from the surface side. It should be noted again that the Zn_2SiO_4 is formed *in the deep region of* SiO_2 *by the implantation*.

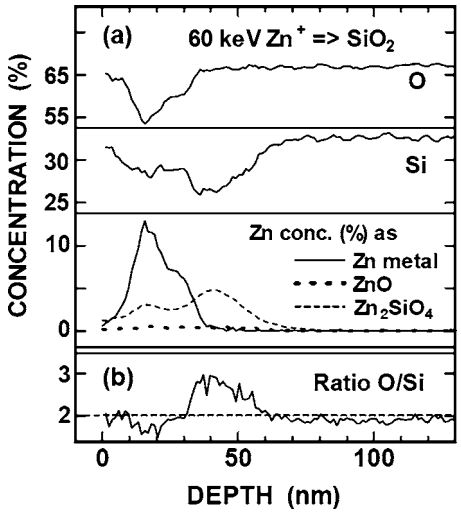

FIG. 3. (a) Concentration profiles of O, Si, and Zn atoms along the depth, determined by XAES and XPS. (b) Numerical ratio of O atoms to Si atoms (N_O/N_{Si}) in SiO_2 implanted with 60 keV Zn^+ ions to a fluence of 1.0×10^{17} ions/cm^2, plotted along the depth.

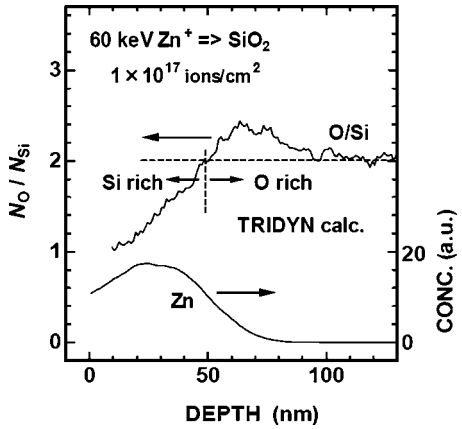

FIG. 4. Numerical ratio of O atoms to Si atoms (N_O/N_{Si}) in SiO_2 implanted with 60 keV Zn^+ ions to a fluence of 1.0×10^{17} ions/cm^2, calculated by TRIDYN code, plotted along the depth. The depth profile of the implanted Zn atoms is also shown.

In addition, a temperature of ~900 °C is necessary for Zn_2SiO_4 formation *under thermal annealing*.[8] At intermediate temperatures of $\sim600<T<\sim800$ °C, the ZnO phase forms instead of Zn_2SiO_4 if a sufficient amount of oxygen is supplied.[8] However, as shown in Fig. 2(a), the ZnO phase is not observed, whereas Zn_2SiO_4 is.

The mean temperature in the implanted layer, attained due to ion beam heating, was estimated taking into account the temperature of the rear surface ($T_o\sim100$ °C) during ion implantation. The temperature increase was estimated as 0.4 °C, using thermal conductivity $\Lambda=0.014$ W/cm K for silica glass around RT.[9] The mean temperature in the implanted layer ($T_o+\Delta T\sim100$ °C) is definitely much lower than the formation temperatures for the ZnO and Zn_2SiO_4 phases, which are ~600 and ~900 °C, respectively.[8]

Figure 3(a) shows depth profiles of Si and O atoms in addition to the profile of Zn atoms. Characteristic differences are observed between the Si and O profiles. While the Si profile has two minima, which correspond to the metallic Zn maximum and the Zn_2SiO_4 maximum, the O profile has only one minimum corresponding to the metallic Zn maximum. The numerical ratio of O atoms to Si atoms is plotted in Fig. 3(b). The region with an O/Si ratio larger than 2 (smaller than 2) corresponds to the O-rich (Si-rich) region in SiO_2. While the depth around the metallic Zn peak is Si rich, the depth around the Zn_2SiO_4 peak is O rich. The inhomogeneous O/Si ratio along the depth is probably a consequence of atomic collisions during the ion implantation in SiO_2. Similar behaviors are reproduced by both the SRIM2003 code[6] and TRIDYN code.[7] The result of TRIDYN calculation is shown in Fig. 4. Si-rich and O-rich regions are formed in the shallow and deep regions, respectively, probably due to the difference in the atomic weights of Si and O atoms. Since O atoms are lighter than Si atoms, the O atoms are displaced to deeper regions than the Si atoms on average.

In the O-rich region, excess O atoms may exist as atomic oxygen, oxygen molecules,[10] or oxygen-excessive defects in the SiO_2 network such as peroxy radicals.[11] These excess O species react with the implanted Zn atoms to form Zn_2SiO_4 via reactions (B) or (C) shown in Table I. However, as already described, the formation of Zn_2SiO_4 requires not only an excess of oxygen but also a temperature of ~900 °C.[4] The rate of formation of Zn_2SiO_4 is probably enhanced in nanoscopic regions of the implanted layer by high-density electron excitation and/or by the high density of local atomic vibrations. Thermal spikes may also enhance the reactivity in complicated ways: Since the melting temperatures of Zn, ZnO, Zn_2SiO_4, and SiO_2 are 420, 1970, 1510, and ~1500 °C, respectively,[9,12] they may melt in thermal spikes (approximately thousand degrees). However, these facts do not mean the formation of Zn_2SiO_4 phase because $\Delta G°(T)$ becomes positive at high temperatures, as shown in Table I. On the decay of the thermal spikes, moderately high temperatures around 1000 °C is locally attained for relatively long time and may enhance the Zn_2SiO_4 formation. These models would be consistent with the lack of the ZnO phase. Because of the enhanced reactivity, once the ZnO phase is formed, most of it is rapidly transformed to the Zn_2SiO_4 phase via the reaction with the SiO_2 matrix, even when the mean temperature of the implanted region is as low as RT.

A part of this study was supported by JSPS-KAKENHI (No. 18510102) and also by the Futaba Electronics Memorial Foundation.

[1] M. Nastasi, J. W. Mayer, and J. K. Hirvonen, *Ion-Solid Interactions: Fundamentals and Applications* (Cambridge University, Cambridge, 1996), Chap. 7.11.
[2] E. L. Williams, J. Am. Ceram. Soc. **48**, 190 (1965).
[3] Y. X. Liu, Y. C. Liu, D. Z. Shen, G. Z. Zhong, X. W. Fan, X. G. Kong, R. Mu, and D. O. Henderson, Solid State Commun. **121**, 531 (2002).
[4] H. Amekura, N. Umeda, Y. Sakuma, O. A. Plaksin, Y. Takeda, N. Kishimoto, and Ch. Buchal, Appl. Phys. Lett. **88**, 153119 (2006).
[5] M. Nagoshi, *X-ray Photoelectron Spectroscopy*, edited by The Surface Science Society of Japan (Tokyo, Maruzen, 1998), p. 137 [in Japanese].
[6] J. F. Ziegler, J. P. Biersack, and U. Littmark, *The Stopping and Range of Ions in Solids* (Pergamon, New York, 1985), Chap. 8.
[7] W. Moeller and W. Eckstein, Nucl. Instrum. Methods Phys. Res. B **9**, 814 (1984).
[8] H. Amekura, K. Kono, N. Kishimoto, and Ch. Buchal, Nucl. Instrum. Methods Phys. Res. B **242**, 96 (2006).
[9] *Tables of Physical Constants*, new ed. (Asakura, Tokyo, 1978) [in Japanese].
[10] L. Skuja and B. Guttler, Phys. Rev. Lett. **77**, 2093 (1996).
[11] D. L. Griscom, J. Ceram. Soc. Jpn. **99**, 923 (1991).
[12] O. Kubaschewski, E. Ll. Evans, and C. B. Alcock, *Metallurgical. Thermochemistry*, 4th ed. (Pergamon, London, 1967), Appendix.